Accepted Manuscript

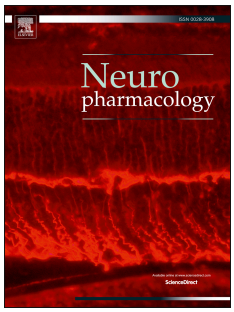

Acid-sensing ion channel (ASIC) structure and function: Insights from spider, snake and sea anemone venoms

Ben Cristofori-Armstrong, Lachlan D. Rash

PII: S0028-3908(17)30192-2

DOI: 10.1016/j.neuropharm.2017.04.042

Reference: NP 6698

To appear in: *Neuropharmacology*

Received Date: 12 February 2017

Revised Date: 7 April 2017

Accepted Date: 27 April 2017

Please cite this article as: Cristofori-Armstrong, B., Rash, L.D., Acid-sensing ion channel (ASIC) structure and function: Insights from spider, snake and sea anemone venoms, *Neuropharmacology* (2017), doi: 10.1016/j.neuropharm.2017.04.042.

Acid-sensing ion channel (ASIC) structure and function: insights from spider, snake and sea anemone venoms.

Ben Cristofori-Armstrong[a,b,*] and Lachlan D. Rash[a,b,*]

[a]Institute for Molecular Bioscience, The University of Queensland, St Lucia, QLD 4072, Australia

[b]School of Biomedical Sciences, The University of Queensland, St Lucia, QLD 4072, Australia

***Address for correspondence**

Dr Lachlan D. Rash: School of Biomedical Sciences, The University of Queensland, St Lucia, QLD 4072, Australia; Phone: +61 7 3346 2985; E-mail: l.rash@uq.edu.au.

Ben Cristofori-Armstrong: Institute for Molecular Bioscience, The University of Queensland, St Lucia, QLD 4072, Australia; Phone: +61 7 3346 2325; E-mail: b.cristoforiarmstrong@uq.edu.au.

ABSTRACT

Acid-sensing ion channels (ASICs) are proton-activated cation channels that are expressed in a variety of neuronal and non-neuronal tissues. As proton-gated channels, they have been implicated in many pathophysiological conditions where pH is perturbed. Venom derived compounds represent the most potent and selective modulators of ASICs described to date, and thus have been invaluable as pharmacological tools to study ASIC structure, function, and biological roles. There are now ten ASIC modulators described from animal venoms, with those from snakes and spiders favouring ASIC1, while the sea anemones preferentially target ASIC3. Some modulators, such as the prototypical ASIC1 modulator PcTx1 have been studied in great detail, while some of the newer members of the club remain largely unstudied. Here we review the current state of knowledge on venom derived ASIC modulators, with a particular focus on their molecular interaction with ASICs, what they have taught us about channel structure, and what they might still reveal about ASIC function and pathophysiological roles.

1. Introduction to acid-sensing ion channels

Acid-sensing ion channels (ASICs) were first discovered at the sequence level in 1996 (Garcia-Anoveros et al., 1997; Price et al., 1996; Waldmann et al., 1996) and shortly thereafter identified as proton-gated cation channels (Waldmann et al., 1997). They are abundantly expressed throughout mammalian neuronal and non-neuronal tissues, where they are primary acid-sensors. There are four human ASIC (hASIC) genes (*ASIC1–4*, renamed from the previous *ACCN* designation) encoding at six major subunits (ASIC1a, ASIC1b, ASIC2a, ASIC2b, ASIC3, and ASIC4). The *ASIC1* and *ASIC2* genes are alternatively spliced to produce "a" and "b" isoforms, which differ in the N-terminal third of the protein (Bässler et al., 2001; Lingueglia et al., 1997). Additionally, there are three functional splice variants of hASIC3 (a, b and c), which do not appear to be present in rodents (Delaunay et al., 2012). Three ASIC subunits combine to form functional homo- and heterotrimers (Jasti et al., 2007) with different biophysical properties and expression profiles (Cristofori-Armstrong et al., 2015; Gründer and Pusch, 2015; Hesselager et al., 2004). The rapid, transient peak-current of ASICs is selective for Na^+ over K^+ by a factor of ~10, and desensitises within seconds in the continued presence of an acidic pH. That is, ion channels enter a non-conducting state and fail to respond to additional acidification (Waldmann et al., 1997). ASIC activation is pH-dependent (i.e., current amplitude increases with decreasing pH until a maximal current amplitude is reached) (Wu et al., 2004). Prolonged exposure of ASICs to mildly acidic pH or slow acidification results in steady-state desensitisation (SSD) without the channel entering an observable open conducting state (Babini et al., 2002). This has been proposed to be due to the rapid kinetics of desensitisation and a slow on-rate for protons at lower concentrations, thereby masking any transition through an open state (Gründer and Pusch, 2015). The model proposed by Gründer and Pusch is however qualitative in nature, and it was noted that the possibility of a simple closed to desensitised transition cannot be excluded. In this alternative, and possibly simplest explanation, the gating of ASICs does allow a direct transition from the closed to the

desensitised state, as desensitisation is more pH-sensitive than activation. In this case, upon slow or mild acidification, the channels would desensitise before activation could take place (thus any observable current). Whereas during rapid acidification, channel activation is observable due to the faster kinetics of activation compared to desensitisation (however channel opening would still be inherently influenced by the rate of desensitisation and likely be underestimated). Nevertheless, the complete picture of ASIC gating remains to be solved and remains an area of intense research interest.

A massive leap in our understanding of the structure of ASICs occurred when the crystal structure of chicken ASIC1 (ASIC1a sequence homologue) was published in 2007 (Jasti et al., 2007), even though the construct used for crystallisation was a non-functional channel with heavily truncated N- and C-termini. The structure revealed the trimeric nature of ASICs, and showed that each subunit consists of short intracellular N- and C-termini and two hydrophobic transmembrane (TM) domains separated by a large extracellular domain of ~370 residues. The structure of an individual subunit was described as resembling a hand clenched around a ball comprising a wrist, palm, finger, knuckle, thumb, and β-ball domains (see Figure 1A). Subsequently a less severely N-terminally truncated and functional cASIC1 construct, named Δ13 cASIC1, was crystallised in the presumed desensitised state and differed from the previous structure primarily in the orientation of the TM domains (Gonzales et al., 2009). Recent cASIC:venom peptide co-crystal structures have provided further insights into ASIC structure and gating and are discussed in Sections 2.1.2 and 2.5.2 (Figure 1C & D).

Despite the growing interest in ASICs, and the increasing volume of work being produced in the field, there are still many unanswered questions. Venom derived compounds have greatly enhanced our understanding of ASICs to date, and are likely to play an important role in the future. In this review, we will focus on our current understanding of these venom-derived compounds, and how they have provided critical information on ASIC structure and function. Please refer to these reviews for more in-depth coverage of recent advances in genetic

models (Lin et al., 2015) and biophysical properties (Gründer and Pusch, 2015) of ASICs, and more comprehensive coverage of the *in vivo* use of ASIC modulating venom peptides to study the pathological roles of ASICs (Baron et al., 2013; Baron and Lingueglia, 2015).

2. Venom peptides targeting ASICs

Many endogenous and exogenous modulators of ASICs have now been discovered, however essentially all the known small molecule ligands are either non-selective and/or lack potency, or are not yet sufficiently characterised (Rash, 2017). Although the lack of truly selective modulators of ASICs has made it difficult to tease out the relative importance of specific ASIC subtypes, the most interesting and selective tools available to date have all come from animal venoms.

2.1. PcTx1

2.1.1. The prototypical, selective ASIC inhibitor

PcTx1 (also known as π-TRTX-Pc1a) is a 40-residue peptide isolated from the venom of the Trinidad chevron tarantula *Psalmopoeus cambridgei* (Escoubas et al., 2000) (Figure 2A). Although isolated as the first highly potent and selective inhibitor of homomeric ASIC1a (rat IC_{50} ~1 nM conditioned at pH 7.45 and human IC_{50} ~3 nM conditioned at pH 7.2), PcTx1 has subsequently been shown to also inhibit currents in ASIC1a/2b co-expressing cells (mouse IC_{50} ~3 nM) and heteromeric rat ASIC1a/2a channels (by ~35–85% at 50 nM conditioned at pH 6.95 depending on trimer composition) (Joeres et al., 2016; Sherwood et al., 2011). At higher concentrations PcTx1 potentiates ASIC1b (rat EC_{50} ~100 nM) (Chen et al., 2006) and is an agonist and/or potentiator of cASIC1 depending on the conditions used (EC_{50} ~10–189 nM) (Hoagland et al., 2010; Smith and Gonzales, 2014). The NMR structure of PcTx1 (Figure 2B), which was first solved in 2003 and further refined in 2011, revealed the presence of an inhibitor cysteine knot (ICK) motif and that the dominant β-hairpin loop (loop 4), which

presents some of the key pharmacophore residues, is highly flexible (Escoubas et al., 2003; Saez et al., 2011).

PcTx1 binds in a state-dependent manner to both ASIC1a and ASIC1b. It acts as a gating modifier of ASIC1a by increasing the channel's apparent affinity for protons, thereby rendering the channel inactive at resting physiological pH of 7.4 (Chen et al., 2005). This effect can be seen as a shift in the steady-state desensitisation (SSD) and activation curves to less acidic pH values. It is in fact this mechanism of action that renders PcTx1 less potent at human as compared to rodent ASIC1a (Sherwood and Askwith, 2008). The SSD of hASIC1a is inherently less sensitive to pH, thus a higher concentration of PcTx1 is required to capture the channel in a desensitised (and non-conducting) state when conditioned at pH 7.4. In agreement with this, mutation of five residues of hASIC1a to the equivalent mouse ASIC1a (mASIC1a) residues makes the pH sensitivity of the species variants equal. This mutant hASIC1a channel regains the same sensitivity to PcTx1 as that of mASIC1a (Sherwood and Askwith, 2008). The potentiation of ASIC1b currents by PcTx1 is due to a large shift in the activation curve to less acidic pH (whereas the SSD curve is largely unaffected) and concomitant slowing of desensitisation as seen by an increase in the decay time constant in the presence of PcTx1 (Chen et al., 2006). The agonist/potentiating effect of PcTx1 on cASIC1 has so far not been studied in much detail but is likely through stabilising the open state of the channel by enhancing activation, slowing desensitisation or both. Interestingly, studies of PcTx1's functional effect on cASIC1 revealed a biphasic response whereby application of PcTx1 at pH 7.35 transiently opened the channel, followed by only partial desensitisation to a long-lasting, persistent current (Smith and Gonzales, 2014). The potentiating effect of PcTx1 at rASIC1b and cASIC1 may be partly explained by the "pH sensor-trapping model" proposed by Salinas et al. (Salinas et al., 2014). Using ASIC chimeras and mutant channels, it was shown that loss of PcTx1 contacts with either the palm and/or β-ball regions of rASIC1a led to current potentiation via movement induced by peptide binding to the thumb domain. This complex

pharmacology shows that PcTx1 can preferentially stabilise several states of ASICs that are dependent on the external environment and inherent gating properties of the channel being studied. It also highlights that very small differences in the molecular interaction between peptide and channel can greatly change the functional effect of a ligand.

The substantial subtype, species, and condition-dependent functional effects of PcTx1 are likely to make it a very difficult peptide to manipulate for use as a truly selective pharmacological tool or therapeutic lead, and also warrant caution when interpreting results from *in vivo* experiments. These factors also warrant caution when interpreting ASIC electrophysiology data. Due to its subtype-dependent effects on channel opening and desensitisation, the rate of solution exchange in experimental setups can have a substantial effect on the observed activity and relative potencies. For example, a slow solution exchange of the recording chamber coupled with recording in large oocyte cells (where much of our PcTx1 information has been derived) could lead to inaccurate interpretation of observations if the peptide application is slower than the inherent gating time scale of the ASIC in question. These are less likely to be issues with fast solution exchange as achieved using whole-cell recordings from small cells or macro-patch recordings. Nevertheless, it is important for authors to include such details when reporting their data, and for readers when assessing the conclusions made about an ASIC modulators functional effects.

Using alanine-scanning mutagenesis of PcTx1 we determined the primary functional pharmacophore at rat (r) ASIC1a to comprise the residues Trp7, Trp24, Phe30, Arg26, Arg27, and Arg28 (Saez et al., 2015; Saez et al., 2011). These findings agree with the co-crystal structures of PcTx1:cASIC1, however the structures showed many more close contacts between the peptide and channel (Baconguis and Gouaux, 2012; Dawson et al., 2012) (Figure 3A–C). From these studies we hypothesise that the peptide binding is largely mediated through the hydrophobic patch comprised of residues Trp7, Trp24, Phe30 (with contributions from the C4 sidechain of R26) while the functional consequence of binding is due to the positively

charged, basic cluster of Arg26, Arg27, and Arg28, that form interactions with proton-sensing residues in the acidic pocket (Saez et al., 2015) (Figure 3B), however, this theory requires some direct binding experiments to confirm. An unexpected outcome of these peptide mutagenesis studies was the discovery of some potent ASIC1a potentiating molecules, the PcTx1 mutants R26A and F30A. The subtype selectivity and mechanism of action of these peptides is yet to be determined, nevertheless they appear to represent new pharmacological tools with activity profiles different to those so far isolated directly from venoms. A combination of approaches employing radioligand binding and electrophysiology with chimeric channels (Chen et al., 2006; Salinas et al., 2006), mutagenesis (Saez et al., 2015) and co-crystal structures (Baconguis and Gouaux, 2012; Dawson et al., 2012) has shown that PcTx1 binds to the acidic pocket with the majority of contacts on the thumb domain, with residues on α helix 5 being particularly critical. The thumb region is known to be important for proton binding and subsequent gating of the channel (Ramaswamy et al., 2013), consistent with PcTx1 mimicking the action of protons and inhibiting ASIC1a via stabilising the desensitised state (Chen et al., 2005).

2.1.2. PcTx1 and structural insights into ASICs

Two groups independently solved the PcTx1-cASIC1 crystal complex in mid 2012 (Baconguis and Gouaux, 2012; Dawson et al., 2012), and these were the first ligand bound structures of ASICs (Figure 1C). Dawson et al. used the non-functional cASIC1 construct at pH 5.5, which resulted in a channel structure almost identical to the apo structure of this construct. This study provided the first detailed picture of the PcTx1 binding site but unfortunately little new information on different channel states. In contrast Baconguis and Gouaux used the Δ13 cASIC1 functional construct (at pH 7.25 and 5.5), and were able to produce crystals in what appear to be two different open conformations. The pH 7.25 structure

was proposed to be non-selective for monovalent cations, whilst the pH 5.5 structure to be Na^+-selective (P_{Na}/P_K = 10/1, i.e. the same selectivity as seen for typical ASIC currents). It remains to be seen if there is any correlation between the two channel states observed independently in the functional studies by Smith and Gonzales (2014) and these structural studies, and what affect the Δ13 truncation has on channel structure-function.

At the time, the low pH structure was proposed to be the 'open' state of the channel. There is very little difference in the extracellular domain between the 'open' and desensitised states, however significant conformational rearrangements occur in the TM domains, as previously predicted from accessibility studies with cysteine-reactive reagents (Li et al., 2011). The available crystallographic data suggested desensitisation gating (open to desensitised transition) to involve binding of stimulatory ligands (protons and/or PcTx1) to the thumb and finger, that results in rotational and flexing movement of the TM domains mediated via the wrist and lower palm. How well these structural rearrangements translate to changes that occur during activation gating remains unexplained. Further details on the structure of the pore and 'open' state of ASICs were revealed when the MitTx-cASIC1 crystal complex was solved two years later in 2014 (See Section 2.4.2).

2.1.3. The neuroprotective properties of PcTx1

Being the first-discovered, selective inhibitor of ASICs, PcTx1 has been extensively used in animals to help determine the role of ASIC1a in a wide variety of physiological and pathological processes such as pain, anxiety, depression, epilepsy (with contrasting results) and respiratory control (Baron et al., 2013; Baron and Lingueglia, 2015; Wemmie et al., 2006; Wemmie et al., 2013). However, the standout condition in which PcTx1 has played a role in validating ASIC1a as a promising therapeutic target is ischaemic stroke. A key role for ASIC1a in the neuronal cell death following ischemic stroke was first reported in 2004 (Xiong et al.,

2004). Xiong and colleagues provided evidence from a combination of genetic and pharmacological approaches using the non-selective ASIC inhibitor amiloride as well as PcTx1. However, instead of using pure peptide, "PcTx1 venom" was employed in both the *in vitro* and *in vivo* aspects of the study. The crude tarantula venom that contains PcTx1 (at only 0.4%) is complex and contains a multitude of other bioactive peptides (see (McCarthy et al., 2015)). "PcTx1 venom" was also used in a follow up study that demonstrated a substantial therapeutic time window for ASIC inhibition (up to five hours post insult) as well as neuroprotective efficacy when delivered intranasally (Pignataro et al., 2007). Pure PcTx1 has since been shown to be neuroprotective in both rodent and porcine models of cerebral ischemia when administered 30 min prior to induction of stroke (Duan et al., 2011; Yang et al., 2011). More recently a study confirmed that a single dose of pure PcTx1 (1 ng/kg, i.c.v. 2 hours post stroke) does indeed provide substantial neuronal and functional protection in ischemic stroke in conscious hypertensive rats (McCarthy et al., 2015). Promisingly, none of the studies using PcTx1 *in vivo* reported any obvious adverse effects let alone acute toxicity, consistent with the original CNS toxicity test in mice by Escoubas et al. (Escoubas et al., 2000). Thus PcTx1 has proved to be an important tool in the identification and confirmation of ASIC1a as a stroke target.

2.2. Hm3a

At the same time as the identification of PcTx1, a second, homologous peptide was identified from tarantula venom (Escoubas unpublished). However, it remained unstudied and unreported until now. In this issue of Neuropharmacology we present the characterisation of π-TRTX-Hm3a (Hm3a) isolated from the Togo starburst tarantula (*Heteroscodra maculata*) (Er et al., 2017). Hm3a has five amino acid substitutions compared to PcTx1 and is shorter by three residues at the C-terminus (Figure 2A). Of these residues, only the R28K substitution lies within the active site, however is a conservative change that has little apparent effect on

potency. To further understand the ASIC1 isoform selectivity and peptide-channel interaction surface for Hm3a and PcTx1, we studied crystal contact residues on the complementary surface to the thumb domain (i.e., the loop between β-strands 3 and 4 in the palm domain of the adjacent subunit). Rat ASIC1a was mutated to mimic ASIC1b within the 19-residue region N-terminal to the ASIC1a/1b splice site known to be crucial for PcTx1 function (Chen et al., 2006; Salinas et al., 2006). Testing of these mutants for sensitivity to PcTx1 identified Arg175 and Glu177 (Cys and Gly in ASIC1b, respectively) to play a key role in the subtype dependent effects of Hm3a. Er et al. also showed that Hm3a potentiates acid-induced currents in oocytes co-injected with rASIC1a and rASIC1b (Er et al., 2017), an effect we observed for PcTx1 (unpublished observations), which has not previously been noted.

Interestingly, this study performed *in vitro* stability assays and revealed that PcTx1 is not as biologically stable as one might assume for an ICK peptide whereas Hm3a is. Hm3a was extremely stable in human serum over 48 hours (~87% remaining), whereas ~35% of PcTx1 remained over the same assay time. Hm3a had very little breakdown over 48 hours at 55 °C, however PcTx1 showed some loss (~24%). The superior stability of Hm3a over PcTx1, coupled with the similar pharmacology of the peptides makes Hm3a a potentially more attractive ASIC tool for *in vivo* studies.

2.3. Hi1a

The recent discovery of a third ASIC inhibitor from spider venom has defined a novel class of ASIC modulatory peptides with unique structural and pharmacological properties. The sequence of Hi1a was noticed during analysis of the venom-gland transcriptome of an Australian funnel-web spider (*Hadronyche infensa*) as its N-terminus bore a striking similarity to PcTx1 (62% identity). However, unlike PcTx1, Hi1a is almost twice the length at 75 residues, with the C-terminal half also resembling PcTx1 (50% identity) (Chassagnon et al., 2017) (Figure 2A). Recombinant production of the peptide allowed structural and functional

studies confirming that Hi1a is indeed a highly potent inhibitor of ASIC1a (IC_{50} of 400–500 pM) and takes the form of two ICK motifs in series (Figure 2B), similar to the TRPV1 agonist DkTx (Bohlen et al., 2010). Despite Hi1a's high sequence identity with PcTx1 and Hm3a, it has a unique pharmacological profile against ASICs. In contrast to the single ICK peptides, which affect ASIC1 desensitisation gating (either facilitating it, ASIC1a, or hindering it, ASIC1b) in a pH-dependent and rapidly reversible manner, Hi1a selectively inhibits the activation of ASIC1a in a slowly reversible manner and has little effect on ASIC1b up to 1 μM. Thus, Hi1a is the most potent and selective inhibitor of ASIC1a discovered to date making it a valuable research tool. Indeed, the initial assessment of its *in vivo* efficacy in ischaemic stroke showed that a single dose of Hi1a (2 ng/kg, i.c.v.) provides a very substantial level of neuroprotection even when administered up to eight hours post-insult. Preliminary structure-activity studies show that the binding site of Hi1a overlaps that of PcTx1 and suggest that the relative orientations of the two knot motifs is important for its unique mechanism and kinetics (Chassagnon et al., 2017). The combined ability of Hi1a to stabilise the resting state of ASIC1a and dissociate slowly suggest that it will be very useful in ASIC structural studies as well as localisation studies of the channel.

2.4. APETx2

2.4.1. The first selective ASIC3 inhibitor

APETx2 is a 42-residue peptide, isolated from extracts of the sea anemone *Anthopleura elegantissima* (Figure 2A). It was the first potent and selective inhibitor of ASIC3-containing channels with an IC_{50} of 63 nM for homomeric rASIC3 and 0.1–2 μM for heteromeric rASIC3 containing channels (Diochot et al., 2004). The peptide is slightly less potent on the human ASIC3 subtype with an IC_{50} of 175 nM. APETx2 inhibits the typical transient acid-induced current and the pH 7.0 evoked window (sustained) current of ASIC3 (Deval et al., 2011), as

well as the alkali-induced current of hASIC3 (Delaunay et al., 2012), but does not inhibit the larger sustained current evoked at pHs lower than 5.0 (Diochot et al., 2004). The structure of APETx2 consists of a compact hydrophobic core composed of a four-stranded β-sheet containing three disulfide bonds, resembling a defensin-like fold (Figure 2B & 3D) (Chagot et al., 2005; Jensen et al., 2014). At higher concentrations APETx2 also inhibits the voltage-gated sodium channels $Na_V1.2$, $Na_V1.6$, and $Na_V1.8$ with varying degrees of potency depending on subtype and study (Blanchard et al., 2012; Peigneur et al., 2012). Additional off target effects have been shown with APETx2 also inhibiting the cardiac hERG channel in the low micromolar range (Jensen et al., 2014), demonstrating that this prototypical "selective" ASIC3 inhibitor is not as selective as at first thought.

The pharmacophore of APETx2 for ASIC3 has recently been shown to comprise a contiguous surface made up of loops 2 and 4 and the N-terminus (Figure 1A, 3D) (Anangi et al., 2012; Jensen et al., 2014). Mutagenesis of APETx2 and its interaction with hERG has also been studied in some detail showing a partial overlap in the pharmacophore with that of ASIC3 (Jensen et al., 2014). Nevertheless, the molecular details of the interaction between APETx2 and ASIC3 (or indeed its off target channels), including the mechanism of action and binding sites have not been extensively studied. It has been speculated that APETx2 binds to the acidic pocket and shifts the channel's apparent affinity for protons (Baron et al., 2013) in the opposite direction to that of PcTx1. More recently a docking study predicted the binding site to be either the upper thumb area, or slightly above the transmembrane domains, between the wrist and palm region (Rahman and Smith, 2014). However, there is currently no published functional evidence to support either of these hypotheses. Given that APETx2 is still the most potent ligand available to study ASIC3, unequivocally determining it binding site and mechanism of action are crucial to develop more selective analogues and further our understanding of ASIC3 structure and *in vivo* function.

2.4.2. An APETx2 analogue from another sea anemone

π-AnmTX Hcr 1b-1 (also Hcr 1b-1) is a peptide related to APETx2 (51% identity, Figure 2A) and was isolated from the sea anemone *Heteractis crispa* (Kozlov et al., 2012). The peptide inhibits the transient current of hASIC3 expressed in *Xenopus* oocytes with an IC_{50} value of 5.5 μM. Although much less potent than APETx2 (~35 fold) and significantly different in sequence, it is interesting to note that the peptides share identity for much of the APETx2 pharmacophore for ASIC3. The sequence differences between these peptides and their comparative activity on APETx2's off targets should provide some novel insight to structural elements that give rise to the ASIC3 activity profile.

2.4.3. APETx2 in peripheral pain

The use of APETx2 *in vivo* has been key in establishing the role of ASIC3 as a sensor of acid-induced and post-operative pain (Deval et al., 2011), and demonstrating its involvement in inflammatory pathways (Deval et al., 2008). In agreement with this, several independent labs have reported that APETx2 is analgesic in rat models of inflammatory and osteoarthritic pain (Deval et al., 2008; Ikeuchi et al., 2009; Karczewski et al., 2010). Peripheral application of APETx2 also reduces mechanical hypersensitivity in non-inflammatory muscular pain models and angina (Ikeuchi et al., 2008; Yagi et al., 2006). In a study assessing the biological stability of APETx2 and cyclised analogues, the wild-type peptide was almost completely broken down in simulated gastric fluid within 20 minutes while the stability in serum was not assessed (Jensen et al., 2012). Despite the promising results from animal pain models, the biological stability and off target profile of APETx2 would appear to greatly restrict its value as a therapeutic lead candidate.

2.5. MitTx

2.5.1. A potent ASIC agonist that causes pain

MitTx was isolated from the Texas coral snake (*Micrurus tener tener*) based on its ability to robustly activate a population of rat cultured sensory neurons (Bohlen et al., 2011). The active toxin is a 1:1 complex of two non-covalently bound subunits — MitTx-α consisting of a 60-residue Kunitz type peptide, and MitTx-β, which is a 120-residue phospholipase A2 (PLA2)-like protein (Figure 2A). Although inactive as individual components, the heterodimer is a potent pH-independent agonist of ASIC1a and ASIC1b (EC_{50} 9 and 23 nM, respectively), whilst being considerably less potent at ASIC3 (EC_{50} 830 nM). MitTx is a weak outright agonist at ASIC2a (i.e., does not directly activate the channel to more than 10% of pH-evoked current size), however it is a strong potentiator of this channel (amplifying the proton-induced current by ~3 orders of magnitude) by shifting the activation curve to more alkaline pH.

The bite of a Texas coral snake is known to be extremely painful, and often requires hospitalisation and administration of opiates (Morgan et al., 2007; Nishioka et al., 1993). Peripheral administration of MitTx into mice hindpaws evoked robust nocifensive responses (Bohlen et al., 2011). This pain behaviour was also observed in $ASIC3^{-/-}$ mice, but not in $ASIC1^{-/-}$ mice. Furthermore, analysis of the MitTx activity in trigeminal neurons from wild-type, $ASIC1^{-/-}$, and $ASIC3^{-/-}$ mice revealed the activation was abolished only in $ASIC1^{-/-}$ animals. These experiments provided the first clear evidence of the involvement of ASIC1 in peripheral nociceptive pathways. Previous studies using PcTx1 and various genetic models have yielded inconsistent phenotypes and somewhat inconclusive results in regards to the role of ASIC1 in peripheral nociception (Lin et al., 2015). Thus, the discovery of the first potent ASIC1 agonist provided a clear leap in knowledge in this field. However, MitTx is a potent agonist of both ASIC1a and ASIC1b channels, making it unclear which subtype is a more important target for peripheral analgesia.

2.5.2. The true open state structure of ASICs?

The most recent structures of cASIC used the Δ13 cASIC1 construct and exploited the fact that it was sensitive to the agonist properties of MitTx (Baconguis et al., 2014). The MitTx-cASIC1 co-crystal complex (Figure 1D) is significantly different to previous ASIC structures in the TM regions, and has been interpreted as the open state that most likely resembles the native Na^+-conducting state. In this structure there is a break in the α helix of the second TM domain (TM2) that causes it to adopt an extended conformation. This structural rearrangement allows the top half of TM2 from one subunit to interact with the bottom half of TM2 from an adjacent subunit (See Figure 1A and 1D). Interestingly, the TM domain swap was also observed in the 2009 desensitised apo structure upon reanalyses of the electron densities (Gonzales et al., 2009), but not in either of the PcTx1 complex structures (Baconguis and Gouaux, 2012). This swapping of TM domains results in a continuous structure that contains a GAS motif that is important for creating the Na^+-selectivity filter of ASICs (Carattino and Della Vecchia, 2012; Kellenberger et al., 2001; Kellenberger et al., 1999; Li et al., 2011). Cs^+-soaked MitTx-cASIC1 crystals revealed coordination of Cs^+ ions by carbonyl atoms of Gly443 of the GAS motif. The pore dimensions in the selectivity filter of these crystals match that of a hydrated Na^+ ion extremely well, suggesting that the TM orientations in this structure may be functionally relevant and provide a barrier mechanism for ion selectivity of ASICs whereby the pore is large enough to admit a hydrated Na^+ ion but exclude a hydrated K^+ ion. This is inconsistent with the findings of Yang and Palmer who, using hASIC1a, showed that when Na^+ is absent, K^+ could freely pass through the channel (Yang and Palmer, 2014). This argues against a barrier mechanism for ion selectivity (or suggests that pore size is not the only factor regulating ion conductance), at least for the human isoform, and highlights that care should be taken when applying observations across specific species or subtype variants of ASICs.

The MitTx-cASIC1 crystal structure not only provided possible further insights into channel gating, but also revealed the expansive MitTx binding site, and both peptide and channel residues that could be functionally critical. In contrast to PcTx1 and mambalgins that bind at

the interface between adjacent subunits, MitTx binds almost exclusively to a single subunit from the wrist to the knuckle, along the entire length of the thumb domain. There is a caveat here in that the cASIC-MitTx complex crystallised as an ASIC monomer (Baconguis et al., 2014) as opposed to a trimer thus there is not much choice but to bind to a single subunit (Baconguis and Gouaux, 2012). Nevertheless, there is an overlap in the binding site of the β subunit of MitTx and PcTx1 at the acidic pocket (Figure 3A), explaining the mutually exclusive functional activity of these peptides observed in earlier studies (Bohlen et al., 2011). The α subunit binds below the β subunit towards the base of the thumb and extracellular domains, another region known to be important for channel gating (Li et al., 2010; Roy et al., 2013; Springauf et al., 2011) (Figure 1D and 3A).

The various crystal structures of ASICs, channel alone and venom peptide bound, have provided valuable insight into the structural basis of channel gating. Nevertheless, many details regarding the gating of ASICs remain to be determined. All ASIC structures solved to date have been of cASIC1, which can be pharmacologically quite different when compared to mammalian ASIC1a despite ~89% sequence identity. For example, the functional effects of PcTx1 are more similar for ASIC1b and cASIC1 than ASIC1a and cASIC1. And more strikingly, 2-guanidine-4-methylquinazoline (GMQ) has the same effect on the pH activation curve of ASIC3 and cASIC1 (shifting to more alkaline values) but the opposite effect on ASIC1a (Alijevic and Kellenberger, 2012; Smith and Gonzales, 2014). Several of the key questions remaining in this area are: *Which ASIC subtype does cASIC1 truly resemble in structure and function, and what does this mean for interpreting data from mammalian channels in light of the cASIC structure? Is there only one true open state, or are there several physiologically relevant open states?* And perhaps the most important unanswered question in regards to ASIC structure and gating: *What is the conformation of the closed/resting state?* As PcTx1 and MitTx have allowed the structural insights into the possible open states described

above, it is likely that a ligand able to stabilise the channel in a closed state would be of great use in this endeavour.

2.6. Mambalgins

2.6.1. Pharmacology and structure of mambalgins

Mambalgins are a group of homologous peptides isolated from the venom of mamba snakes. Two 57-residue peptides were isolated from the black mamba (*Dendroaspis polylepsis polylepsis*) that differ by one amino acid have been named mambalgin-1 and mambalgin-2 (Ma-1 and Ma-2, respectively) (Diochot et al., 2012). A third peptide, Ma-3, from the green mamba (*Dendroaspis augusticeps*) was also isolated and has a single mutation at position 23 when compared to Ma-1 (Baron et al., 2013) (Figure 2A). These peptides conform to the three-finger toxin fold (Figure 2B) and inhibit homomeric ASIC1a (rat and human IC_{50} 3–55 and 127 nM, respectively) and rASIC1b (IC_{50} 44–192 nM), as well as ASIC1a- and ASIC1b-containing heteromers with weaker potency (Diochot et al., 2012; Mourier et al., 2016; Schroeder et al., 2014). Mambalgins inhibit ~60% of ASIC currents in rat sensory neurons, whereas PcTx1 only inhibits ~40%, most likely due to the broader activity profile of mambalgins through ASIC1b containing channels (Diochot et al., 2012). A study using human stem cell-derived sensory neurons showed that Ma-1 also inhibits native human ASIC currents (Young et al., 2014). Although there are small discrepancies in the potency of peptides across platforms and publications, all three peptides have been reported to have the same overall pharmacological profile.

Mambalgins are thought to preferentially bind to the closed state of ASICs and inhibit channels by shifting the pH-dependence of activation to more acidic pH, decreasing their apparent affinity for protons (Diochot et al., 2016; Salinas et al., 2014). Chimeric studies in which domains of ASIC1a were swapped with ASIC2a (not sensitive to mambalgins) suggest that the mambalgins bind in the region of the acidic pocket, with the peptide interacting with

the β-ball and upper thumb of one subunit and the palm of the adjacent subunit (Salinas et al., 2014). Single point mutants of the channel in this region were also made to identify specific interacting residues of which F350 on helix 5 in the thumb stands out as an important contact (Salinas et al., 2014; Schroeder et al., 2014). However, these studies lack the detail to explain the observed selectivity/potency differences between ASIC species isoform and subtypes. The pharmacophore of Ma-1 has also been partially determined with alanine mutants only made so far in loop 2. Mutating residues Phe27, Arg28, Leu32, Ile33, and Leu34 induced a significant decrease in potency, and this face of the peptide was determined to be the ASIC-interacting surface (Mourier et al., 2016) (Figure 3F), in contrast to the results of a prior docking-based prediction by the same group (Salinas et al., 2014).

Unlike PcTx1 and APETx2, recombinant production of mambalgins has not been reported. However several elegant strategies have been developed to synthesise the peptide for structural and functional studies (Mourier et al., 2016; Pan et al., 2014; Schroeder et al., 2014). Two high-resolution NMR structures have been published and are in good agreement with one another, with the lower part of loop 2 showing some flexibility within the NMR ensemble (Pan et al., 2014; Schroeder et al., 2014). More recently crystal structures of two Ma-1 polymorphs were determined, showing significant structural variations compared to the NMR structures (Mourier et al., 2016) (see Figure 2B). In both crystal structures the lower part of loop 2 is extended and well defined and there was a large degree of conformational variability in loop 3. Of the two crystal structures, the most frequently observed and most ordered conformation of loop 3 was a single-turn helix. The NMR structures of this region contain a short β-sheet, and this conformation can also be seen as a less frequent form within the crystal structures. It must also be noted that for both polymorphs of the wild-type peptide, the Ma-1 molecules assembled together as complexes of either dimers or tetramers in a single asymmetric unit. In both crystals there were significant inter-molecular interactions present, which may explain the differences to the more flexible NMR structures, and this may result in structures where the

Ma-1 loops have been stabilised in non-physiologically relevant conformations. These differences between the NMR and crystal structures are extremely important when studying the functional surface of the peptide, as they yield different surface-exposed residues. This will have profound implications when mapping on pharmacophore residues and understanding the nature of the interaction of these peptides with ASICs. Unfortunately, no co-crystal structure of mambalgins in complex with ASICs has been reported to date. Either structural information of the mambalgin-ASIC interaction, or more extensive peptide and channel mutagenesis will be required to truly understand this interaction to facilitate design of ASIC1a or ASIC1b selective analogues.

2.6.2. Is ASIC1b or ASIC1a important in peripheral nociception?

The discovery that MitTx robustly elicits nocifensive (pain-related) behaviour in mice upon intraplantar injection highlighted ASIC1 as an important mediator of peripheral nociception. However, the lack of selective inhibitors of ASIC1b, and lack of peripheral analgesic activity of PcTx1 (Mazzuca et al., 2007) made it difficult to tease out the relative importance of ASIC1a and ASIC1b in peripheral pain. Ma-1 was found to be analgesic when administered centrally or peripherally and experiments with ASIC knockout and knockdown animals suggest that the central effects of Ma-1 are mediated by ASIC1a, whereas peripheral analgesia is mediated by ASIC1b (Diochot et al., 2012). This group has now demonstrated the analgesic potential of mambalgins in rodent models of thermal, inflammatory and neuropathic pain, however this finding has yet to be reported by any independent group (Diochot et al., 2016; Diochot et al., 2012).

2.7. Ugr 9-1

Sea anemones have proved to be a consistent source of ASIC ligands with the painted anemone (*Urticina grebelnyi)* yielding Ugr 9-1 (also π-AnmTx Ugr 9a-1) (Figure 2A), a low

affinity inhibitor of both transient and sustained current of hASIC3 (Osmakov et al., 2013). The peptide reversibly and completely blocked the transient current with an IC_{50} of 10 μM, and inhibited the sustained current with maximal inhibition of ~48% and an IC_{50} of ~1.4 μM. No activity was observed at up to 50 μM on ASIC1a, ASIC1b, and ASIC2a, potentially making it a more selective ASIC3 inhibitor than APETx2. In this study the peptide was applied for only 10 s before the low pH stimulus, thus, depending on its on-rate the IC_{50} values determined could be underestimating the true potency (i.e. if steady-state inhibition is not reached within the short application time used). The peptide was successfully produced in *E. coli* to assist in structure determination and animal studies with a final yield of ~8 mg of peptide per litre of culture. The NMR structure revealed a novel scaffold for short peptides named the boundless β-hairpin. The Ugr 9-1 structure is 'boundless' as the disulfide bonds do not stabilise the core of the peptide (no interstrand disulfides), instead one disulfide links the N-terminus to the β-core, and another the C-terminus to a β-turn (see Figure 2B).

Assessment of the Ugr 9-1 three dimensional surface, and sequence comparison with the ASIC3 inactive homologs Ugr 9-2 and Ugr 9-3 led Osmakov et al. to predict the functional surface to contain Phe9, His12, and Tyr24 of Ugr 9-1 (as these are the only three residues that are unique to Ugr 9-1 when compared to Ugr 9-2 and Ugr 9-3) (Osmakov et al., 2013). Follow up work from the same laboratory introduced the individual mutations T9F and Y12H into the inactive Ugr 9-2 to resemble the active Ugr 9-1 (Osmakov et al., 2016). The mutant peptides gained ASIC3 activity but were 2.2- and 1.3-fold weaker than native Ugr 9-1, respectively, demonstrating the importance of these residues for inhibitory activity. An N- and C-terminally truncated analogue of Ugr 9-1, Ugr22, was also produced and shown to be equipotent with native Ugr 9-1 at inhibiting ASIC3. The mechanism of action and binding site of these peptides is still unknown.

Ugr 9-1 showed analgesic effects in two models of inflammatory pain, the CFA-induced thermal hyperalgesia model, and the acetic acid writhing test (Osmakov et al., 2013). Unsurprisingly, neither of the ASIC inactive peptides Ugr 9-2 and Ugr 9-3 had any effect in the hyperalgesia model. Animals treated with any of the three active peptides showed no motor impairment or sedation, making Ugr 9-1 and Ugr22 promising tools to study ASIC3 *in vivo*. Despite their comparable potency at ASIC3, Ugr22 reversed thermal hyperalgesia with greater efficacy than Ugr 9-1 at 0.1 mg/kg dose (Osmakov et al., 2016) possibly due to the smaller mass of Ugr22, therefore higher molar dose.

2.8. PhcrTx1

PhcrTx1 (also π-PMTX-Pcf1a) was isolated from the sea anemone *Phymanthus crucifer* as an inhibitor of ASIC currents in rat DRG neurons with an IC_{50} ~100 nM (Rodríguez et al., 2014). It also partially (less than 20%) inhibits voltage-gated K^+ currents in DRG neurons in the low micromolar range (IC_{50} ~3.5 μM). PhcrTx1 is a partial inhibitor of the native ASICs currents with maximal inhibition of ~44% at 10 μM. PhcrTx1 is fully reversible within 5 minutes, did not affect the current desensitization rate, and was not active when applied only with the stimulus pH. This suggests the peptide preferentially binds to the closed state of ASICs and prevents activation, potentially providing another novel tool to help understand channel gating. Given the relative potency in inhibiting ASIC currents in rat DRGs, it would be of interest to determine the subtype selectivity of PhcrTx1 and its analgesic potential. PhcrTx1 appears to be the first ICK peptide isolated from sea anemones and only shares 32% identity with PcTx1 (Figure 2A), however the structure or disulfide bond connectivity have not yet been determined experimentally. Nevertheless, molecular modeling of PhcrTx1, calculation of the dipole moment, and comparison with the PcTx1 pharmacophore led the Rodríguez et al. to

predict a cluster of basic/aromatic residues to be the functional site for ASIC activity (Rodríguez et al., 2014).

2.9. α-Dendrotoxin

α-Dendrotoxin (α-DTx) is another toxin isolated from the green mamba venom (same source as Ma-3), and is a well-known low nanomolar K_V1.x channel blocker that was recently shown to also inhibit ASICs with weaker potency (Báez et al., 2015). The 59 amino acid peptide is a single Kunitz domain fold (Skarżyński, 1992), similar to the α-subunit of MitTx. They only share ~32% identity and 55% similarity, however four of the six identified crystal contacts for MitTx are similar in α-DTx raising the possibility that they may bind to a similar site on ASICs (albeit with different functional outcomes). α-DTx reversibly inhibited ASIC peak currents in rat DRG neurons with an IC_{50} of 800 nM. Although the binding site and mechanism of action have yet to be determined, α-DTx inhibition was only present when cells were preconditioned with peptide (applied for 20 s during conditioning at pH 7.4, and also for 5 s during the pH 6.1 acid pulse), but not when applied only with the stimulating pH. This may suggest that α-DTx preferentially binds to the closed state of the channel and prevents activation.

3. Conclusions

Since the discovery of PcTx1 at the turn of the millennium, our understanding of ASIC modulating venom peptides themselves, and their use in deciphering ASIC structure-function and involvement pathological processes have greatly increased. It is now quite clear that as for many other ion channel families, animal venoms are a rich source of potent and valuable ASIC modulators. As detailed above, there are now ten known ASIC modulators from venoms (not including close homologs), so far from only three sources, spiders, sea anemones (the most

prolific source to date) and snakes. Despite this relatively low number (when compared to the number of venom peptides known to modulate Na_V or K_V channels), a trend is starting to appear. The modulators from snakes and spiders are, so far, relatively selective for ASIC1, while the sea anemone peptides seem to preferentially target ASIC3. Whether this holds true over the years to come and what it means from an ecological point of view remain to be seen. Whether venoms will harbour any components that have selectivity for ASIC2 (which to date suffers a dearth of selective tools) also remains to be seen. In the mean time we still have a lot to learn about the tools described above in order to maximise their value as research tools.

Essentially all small molecule modulators of ASICs characterised have poor selectivity against ASIC subtypes. Given the sometimes extensive interaction surface and multi-domain nature of venom peptide binding, we believe these gifts from nature are our best chance at discovering and developing more selective pharmacological tools that can better discriminate between ASIC subtypes. Gaining a thorough understanding of the molecular interactions between selective venom peptides and ASICs will almost certainly facilitate answering some of the major unresolved questions in the ASIC field and may even lead to some novel therapeutics along the way.

Funding

Work in the laboratory of L.D.R. was supported by grants from Australian National Health and Medical Research Council (NHMRC APP1067940; L.D.R.), and B. C-A. is supported by an Australian Postgraduate Award.

Conflict(s) of interest

None.

Acknowledgements

We thank all current and former members of the Rash lab for helpful discussion and comments.

References

Alijevic, O., Kellenberger, S., 2012. Subtype-specific modulation of acid-sensing ion channel (ASIC) function by 2-guanidine-4-methylquinazoline. J. Biol. Chem. 287, 36059-36070.

Anangi, R., Rash, L. D., Mobli, M., King, G. F., 2012. Functional expression in Escherichia coli of the disulfide-rich sea anemone peptide APETx2, a potent blocker of acid-sensing ion channel 3. Mar. Drugs 10, 1605-1618.

Babini, E., Paukert, M., Geisler, H. S., Gründer, S., 2002. Alternative splicing and interaction with di- and polyvalent cations control the dynamic range of acid-sensing ion channel 1 (ASIC1). J. Biol. Chem. 277, 41597-41603.

Baconguis, I., Bohlen, C. J., Goehring, A., Julius, D., Gouaux, E., 2014. X-ray structure of acid-sensing ion channel 1-snake toxin complex reveals open state of a Na(+)-selective channel. Cell 156, 717-729.

Baconguis, I., Gouaux, E., 2012. Structural plasticity and dynamic selectivity of acid-sensing ion channel-spider toxin complexes. Nature 489, 400–405.

Báez, A., Salceda, E., Fló, M., Graña, M., Fernández, C., Vega, R., Soto, E., 2015. α-Dendrotoxin inhibits the ASIC current in dorsal root ganglion neurons from rat. Neurosci. Lett. 606, 42-47.

Baron, A., Diochot, S., Salinas, M., Deval, E., Noël, J., Lingueglia, E., 2013. Venom toxins in the exploration of molecular, physiological and pathophysiological functions of acid-sensing ion channels. Toxicon 75, 187-204.

Baron, A., Lingueglia, E., 2015. Pharmacology of acid-sensing ion channels - Physiological and therapeutical perspectives. Neuropharmacology 94, 19-35.

Bässler, E. L., Ngo-Anh, T. J., Geisler, H. S., Ruppersberg, J. P., Gründer, S., 2001. Molecular and functional characterization of acid-sensing ion channel (ASIC) 1b. J. Biol. Chem. 276, 33782-33787.

Blanchard, M. G., Rash, L. D., Kellenberger, S., 2012. Inhibition of voltage-gated Na(+) currents in sensory neurones by the sea anemone toxin APETx2. Br. J. Pharmacol. 165, 2167-2177.

Bohlen, C. J., Chesler, A. T., Sharif-Naeini, R., Medzihradszky, K. F., Zhou, S., King, D., Sánchez, E. E., Burlingame, A. L., Basbaum, A. I., Julius, D., 2011. A heteromeric Texas coral snake toxin targets acid-sensing ion channels to produce pain. Nature 479, 410-414.

Bohlen, C. J., Priel, A., Zhou, S., King, D., Siemens, J., Julius, D., 2010. A bivalent tarantula toxin activates the capsaicin receptor, TRPV1, by targeting the outer pore domain. Cell 141, 834-845.

Carattino, M. D., Della Vecchia, M. C., 2012. Contribution of residues in second transmembrane domain of ASIC1a protein to ion selectivity. J. Biol. Chem. 287, 12927-12934.

Chagot, B., Escoubas, P., Diochot, S., Bernard, C., Lazdunski, M., Darbon, H., 2005. Solution structure of APETx2, a specific peptide inhibitor of ASIC3 proton-gated channels. Protein Sci. 14, 2003-2010.

Chassagnon, I. R., McCarthy, C. A., Chin, Y. K., Pineda, S. S., Keramidas, A., Mobli, M., Pham, V., De Silva, T. M., Lynch, J. W., Widdop, R. E., Rash, L. D., King, G. F., 2017.

Potent neuroprotection after stroke afforded by a double-knot spider-venom peptide that inhibits acid-sensing ion channel 1a. Proc. Natl. Acad. Sci. USA 114, 3750-3755.

Chen, X., Kalbacher, H., Gründer, S., 2005. The tarantula toxin psalmotoxin 1 inhibits acid-sensing ion channel (ASIC) 1a by increasing its apparent H^+ affinity. J. Gen. Physiol. 126, 71–79.

Chen, X., Kalbacher, H., Gründer, S., 2006. Interaction of acid-sensing ion channel (ASIC) 1 with the tarantula toxin psalmotoxin 1 is state dependent. J. Gen. Physiol. 127, 267–276.

Cristofori-Armstrong, B., Soh, M. S., Talwar, S., Brown, D. L., Griffin, J. D., Dekan, Z., Stow, J. L., King, G. F., Lynch, J. W., Rash, L. D., 2015. Xenopus borealis as an alternative source of oocytes for biophysical and pharmacological studies of neuronal ion channels. Sci. Rep. 5, 14763.

Dawson, R. J. P., Benz, J., Stohler, P., Tetaz, T., Joseph, C., Huber, S., Schmid, G., Hügin, D., Pflimlin, P., Trube, G., Rudolph, M. G., Hennig, M., Ruf, A., 2012. Structure of the acid-sensing ion channel 1 in complex with the gating modifier psalmotoxin 1. Nat. Comm. 3, 936.

Delaunay, A., Gasull, X., Salinas, M., Noel, J., Friend, V., Lingueglia, E., Deval, E., 2012. Human ASIC3 channel dynamically adapts its activity to sense the extracellular pH in both acidic and alkaline directions. Proc. Natl. Acad. Sci. USA 109, 13124-13129.

Deval, E., Noël, J., Gasull, X., Delaunay, A., Alloui, A., Friend, V., Eschalier, A., Lazdunski, M., Lingueglia, E., 2011. Acid-sensing ion channels in postoperative pain. J. Neurosci. 31, 6059-6066.

Deval, E., Noël, J., Lay, N., Alloui, A., Diochot, S., Friend, V., Jodar, M., Lazdunski, M., Lingueglia, E., 2008. ASIC3, a sensor of acidic and primary inflammatory pain. EMBO J. 27, 3047-3055.

Diochot, S., Alloui, A., Rodrigues, P., Dauvois, M., Friend, V., Aissouni, Y., Eschalier, A., Lingueglia, E., Baron, A., 2016. Analgesic effects of mambalgin peptide inhibitors of acid-sensing ion channels in inflammatory and neuropathic pain. Pain 157, 552-559.

Diochot, S., Baron, A., Rash, L. D., Deval, E., Escoubas, P., Scarzello, S., Salinas, M., Lazdunski, M., 2004. A new sea anemone peptide, APETx2, inhibits ASIC3, a major acid-sensitive channel in sensory neurons. EMBO J. 23, 1516-1525.

Diochot, S., Baron, A., Salinas, M., Douguet, D., Scarzello, S., Dabert-Gay, A.-S., Debayle, D., Friend, V., Alloui, A., Lazdunski, M., Lingueglia, E., 2012. Black mamba venom peptides target acid-sensing ion channels to abolish pain. Nature 490, 552-555.

Duan, B., Wang, Y. Z., Yang, T., Chu, X. P., Yu, Y., Huang, Y., Cao, H., Hansen, J., Simon, R. P., Zhu, M. X., Xiong, Z. G., Xu, T. L., 2011. Extracellular spermine exacerbates ischemic neuronal injury through sensitization of ASIC1a channels to extracellular acidosis. J. Neurosci. 31, 2101–2112.

Er, S. Y., Cristofori-Armstrong, B., Escoubas, P., Rash, L. D., 2017. Discovery and molecular interaction studies of a highly stable, tarantula peptide modulator of acid-sensing ion channel 1. Neuropharmacology.

Escoubas, P., Bernard, C., Lambeau, G., Lazdunski, M., Darbon, H., 2003. Recombinant production and solution structure of PcTx1, the specific peptide inhibitor of ASIC1a proton-gated cation channels. Prot. Sci. 12, 1332–1343.

Escoubas, P., De Weille, J. R., Lecoq, A., Diochot, S., Waldmann, R., Champigny, G., Moinier, D., Ménez, A., Lazdunski, M., 2000. Isolation of a tarantula toxin specific for a class of proton-gated Na^+ channels. J. Biol. Chem. 275, 25116–25121.

Garcia-Anoveros, J., Derfler, B., Neville-Golden, J., Hyman, B. T., Corey, D. P., 1997. BNaC1 and BNaC2 constitute a new family of human neuronal sodium channels related to degenerins and epithelial sodium channels. Proc. Natl. Acad. Sci. USA 94, 1459–1464.

Gonzales, E. B., Kawate, T., Gouaux, E., 2009. Pore architecture and ion sites in acid-sensing ion channels and P2X receptors. Nature 460, 599-604.

Gründer, S., Pusch, M., 2015. Biophysical properties of acid-sensing ion channels (ASICs). Neuropharmacology 94, 9-18.

Hesselager, M., Timmermann, D. B., Ahring, P. K., 2004. pH dependency and desensitization kinetics of heterologously expressed combinations of acid-sensing ion channel subunits. J. Biol. Chem. 279, 11006–11015.

Hoagland, E. N., Sherwood, T. W., Lee, K. G., Walker, C. J., Askwith, C. C., 2010. Identification of a calcium permeable human acid-sensing ion channel 1 transcript variant. J. Biol. Chem. 285, 41852–41862.

Ikeuchi, M., Kolker, S. J., Burnes, L. A., Walder, R. Y., Sluka, K. A., 2008. Role of ASIC3 in the primary and secondary hyperalgesia produced by joint inflammation in mice. Pain 137, 662-669.

Ikeuchi, M., Kolker, S. J., Sluka, K. A., 2009. Acid-sensing ion channel 3 expression in mouse knee joint afferents and effects of carrageenan-induced arthritis. J. Pain 10, 336-342.

Jasti, J., Furukawa, H., Gonzales, E. B., Gouaux, E., 2007. Structure of acid-sensing ion channel 1 at 1.9 Å resolution and low pH. Nature 449, 316–323.

Jensen, J. E., Cristofori-Armstrong, B., Anangi, R., Rosengren, K. J., Lau, C. H., Mobli, M., Brust, A., Alewood, P. F., King, G. F., Rash, L. D., 2014. Understanding the molecular basis of toxin promiscuity: the analgesic sea anemone peptide APETx2 interacts with acid-sensing ion channel 3 and hERG channels via overlapping pharmacophores. J. Med. Chem. 57, 9195-9203.

Jensen, J. E., Mobli, M., Brust, A., Alewood, P. F., King, G. F., Rash, L. D., 2012. Cyclisation increases the stability of the sea anemone peptide APETx2 but decreases its activity at acid-sensing ion channel 3. Mar. Drugs 10, 1511-1527.

Joeres, N., Augustinowski, K., Neuhof, A., Assmann, M., Grunder, S., 2016. Functional and pharmacological characterization of two different ASIC1a/2a heteromers reveals their sensitivity to the spider toxin PcTx1. Sci. Rep. 6, 27647.

Karczewski, J., Spencer, R. H., Garsky, V. M., Liang, A., Leitl, M. D., Cato, M. J., Cook, S. P., Kane, S., Urban, M. O., 2010. Reversal of acid-induced and inflammatory pain by the selective ASIC3 inhibitor, APETx2. Br. J. Pharmacol. 161, 950-960.

Kellenberger, S., Auberson, M., Gautschi, I., Schneeberger, E., Schild, L., 2001. Permeability properties of ENaC selectivity filter mutants. J. Gen. Physiol. 118, 679-692.

Kellenberger, S., Gautschi, I., Schild, L., 1999. A single point mutation in the pore region of the epithelial Na+ channel changes ion selectivity by modifying molecular sieving. Proc. Natl. Acad. Sci. USA 96, 4170-4175.

Kozlov, S. A., Osmakov, D. I., Andreev Ia, A., Koshelev, S. G., Gladkikh, I. N., Monastyrnaia, M. M., Kozlovskaia, E. P., Grishin, E. V., 2012. [Polypeptide toxin from sea anemone inhibiting proton-sensitive channel ASIC3]. Bioorg. Khim. 38, 653-659.

Li, T., Yang, Y., Canessa, C. M., 2010. Leu85 in the beta1-beta2 linker of ASIC1 slows activation and decreases the apparent proton affinity by stabilizing a closed conformation. J. Biol. Chem. 285, 22706-22712.

Li, T., Yang, Y., Canessa, C. M., 2011. Outlines of the pore in open and closed conformations describe the gating mechanism of ASIC1. Nat. Commun. 2, 399.

Lin, S. H., Sun, W. H., Chen, C. C., 2015. Genetic exploration of the role of acid-sensing ion channels. Neuropharmacology 94, 99-118.

Lingueglia, E., de Weille, J. R., Bassilana, F., Heurteaux, C., Sakai, H., Waldmann, R., Lazdunski, M., 1997. A modulatory subunit of acid sensing ion channels in brain and dorsal root ganglion cells. J. Biol. Chem. 272, 29778-29783.

Mazzuca, M., Heurteaux, C., Alloui, A., Diochot, S., Baron, A., Voilley, N., Blondeau, N., Escoubas, P., Gelot, A., Cupo, A., Zimmer, A., Zimmer, A. M., Eschalier, A., Lazdunski, M., 2007. A tarantula peptide against pain via ASIC1a channels and opioid mechanisms. Nat. Neurosci. 10, 943-945.

McCarthy, C. A., Rash, L. D., Chassagnon, I. R., King, G. F., Widdop, R. E., 2015. PcTx1 affords neuroprotection in a conscious model of stroke in hypertensive rats via selective inhibition of ASIC1a. Neuropharmacology 99, 650-657.

Morgan, D. L., Borys, D. J., Stanford, R., Kjar, D., Tobleman, W., 2007. Texas coral snake (Micrurus tener) bites. South Med. J. 100, 152-156.

Mourier, G., Salinas, M., Kessler, P., Stura, E. A., Leblanc, M., Tepshi, L., Besson, T., Diochot, S., Baron, A., Douguet, D., Lingueglia, E., Servent, D., 2016. Mambalgin-1 Pain-relieving Peptide, Stepwise Solid-phase Synthesis, Crystal Structure, and Functional Domain for Acid-sensing Ion Channel 1a Inhibition. J. Biol. Chem. 291, 2616-2629.

Nishioka, S. A., Silveira, P. V., Menzes, L. B., 1993. Coral snake bite and severe local pain. Ann. Trop. Med. Parasitol. 87, 429-431.

Osmakov, D. I., Koshelev, S. G., Andreev, Y. A., Dyachenko, I. A., Bondarenko, D. A., Murashev, A. N., Grishin, E. V., Kozlov, S. A., 2016. Conversed mutagenesis of an inactive peptide to ASIC3 inhibitor for active sites determination. Toxicon 116, 11-16.

Osmakov, D. I., Kozlov, S. A., Andreev, Y. A., Koshelev, S. G., Sanamyan, N. P., Sanamyan, K. E., Dyachenko, I. A., Bondarenko, D. A., Murashev, A. N., Mineev, K. S., Arseniev, A. S., Grishin, E. V., 2013. Sea anemone peptide with uncommon beta-hairpin structure inhibits acid-sensing ion channel 3 (ASIC3) and reveals analgesic activity. J. Biol. Chem. 288, 23116-23127.

Pan, M., He, Y., Wen, M., Wu, F., Sun, D., Li, S., Zhang, L., Li, Y., Tian, C., 2014. One-pot hydrazide-based native chemical ligation for efficient chemical synthesis and structure determination of toxin Mambalgin-1. Chem. Commun. (Camb) 50, 5837-5839.

Peigneur, S., Beress, L., Moller, C., Mari, F., Forssmann, W. G., Tytgat, J., 2012. A natural point mutation changes both target selectivity and mechanism of action of sea anemone toxins. FASEB J. 26, 5141-5151.

Pignataro, G., Simon, R. P., Xiong, Z.-G., 2007. Prolonged activation of ASIC1a and the time window for neuroprotection in cerebral ischaemia. Brain 130, 151-158.

Price, M. P., Snyder, P. M., Welsh, M. J., 1996. Cloning and expression of a novel human brain Na+ channel. J. Biol. Chem. 271, 7879-7882.

Rahman, T., Smith, E. S., 2014. In silico assessment of interaction of sea anemone toxin APETx2 and acid sensing ion channel 3. Biochem. Biophys. Res. Commun. 450, 384-389.

Ramaswamy, S. S., MacLean, D. M., Gorfe, A. A., Jayaraman, V., 2013. Proton-mediated conformational changes in an acid-sensing ion channel. J. Biol. Chem. 288, 35896–35903.

Rash, L. D., 2017. Acid-sensing ion channel pharmacology, Past, Present, and Future…. In: Geraghty, D., Rash, L. D., (Eds), Ion Channels DownUnder. Elsevier.

Rodríguez, A. A., Salceda, E., Garateix, A. G., Zaharenko, A. J., Peigneur, S., López, O., Pons, T., Richardson, M., Díaz, M., Hernández, Y., Ständker, L., Tytgat, J., Soto, E., 2014. A novel sea anemone peptide that inhibits acid-sensing ion channels. Peptides 53, 3-12.

Roy, S., Boiteux, C., Alijevic, O., Liang, C., Bernèche, S., Kellenberger, S., 2013. Molecular determinants of desensitization in an ENaC/degenerin channel. FASEB J. 27, 5034-5045.

Saez, N. J., Deplazes, E., Cristofori-Armstrong, B., Chassagnon, I. R., Lin, X., Mobli, M., Mark, A. E., Rash, L. D., King, G. F., 2015. Molecular dynamics and functional studies define a hot spot of crystal contacts essential for PcTx1 inhibition of acid-sensing ion channel 1a. Br. J. Pharmacol. 172, 4985-4995.

Saez, N. J., Mobli, M., Bieri, M., Chassagnon, I. R., Malde, A. K., Gamsjaeger, R., Mark, A. E., Gooley, P. R., Rash, L. D., King, G. F., 2011. A dynamic pharmacophore drives the interaction between psalmotoxin-1 and the putative drug target acid-sensing ion channel 1a. Mol. Pharmacol. 80, 796–808.

Salinas, M., Besson, T., Delettre, Q., Diochot, S., Boulakirba, S., Douguet, D., Lingueglia, E., 2014. Binding site and inhibitory mechanism of the mambalgin-2 pain-relieving peptide on acid-sensing ion channel 1a. J. Biol. Chem. 289, 13363-13373.

Salinas, M., Rash, L. D., Baron, A., Lambeau, G., Escoubas, P., Lazdunski, M., 2006. The receptor site of the spider toxin PcTx1 on the proton-gated cation channel ASIC1a. J. Physiol. 570, 339-354.

Schroeder, C. I., Rash, L. D., Vila-Farrés, X., Rosengren, K. J., Mobli, M., King, G. F., Alewood, P. F., Craik, D. J., Durek, T., 2014. Chemical synthesis, 3D structure, and ASIC binding site of the toxin mambalgin-2. Angew. Chem. Int. Ed. Engl. 53, 1017-1020.

Sherwood, T. W., Askwith, C. C., 2008. Endogenous arginine-phenylalanine-amide-related peptides alter steady-state desensitization of ASIC1a. J. Biol. Chem. 283, 1818-1830.

Sherwood, T. W., Lee, K. G., Gormley, M. G., Askwith, C. C., 2011. Heteromeric acid-sensing ion channels (ASICs) composed of ASIC2b and ASIC1a display novel channel properties and contribute to acidosis-induced neuronal death. J. Neurosci. 31, 9723–9734.

Skarżyński, T., 1992. Crystal structure of α-dendrotoxin from the green mamba venom and its comparison with the structure of bovine pancreatic trypsin inhibitor. J. Mol. Biol. 224, 671-683.

Smith, R. N., Gonzales, E. B., 2014. Protons and Psalmotoxin-1 reveal nonproton ligand stimulatory sites in chicken acid-sensing ion channel: Implication for simultaneous modulation in ASICs. Channels (Austin) 8, 49-61.

Springauf, A., Bresenitz, P., Gründer, S., 2011. The interaction between two extracellular linker regions controls sustained opening of acid-sensing ion channel 1. J. Biol. Chem. 286, 24374-24384.

Waldmann, R., Champigny, G., Bassilana, F., Heurteaux, C., Lazdunski, M., 1997. A proton-gated cation channel involved in acid-sensing. Nature 386, 173–177.

Waldmann, R., Champigny, G., Voilley, N., Lauritzen, I., Lazdunski, M., 1996. The mammalian degenerin MDEG, an amiloride-sensitive cation channel activated by mutations causing neurodegeneration in Caenorhabditis elegans. J. Biol. Chem. 271, 10433-10436.

Wemmie, J. A., Price, M. P., Welsh, M. J., 2006. Acid-sensing ion channels: advances, questions and therapeutic opportunities. Trends neurosci. 29, 578-586.

Wemmie, J. A., Taugher, R. J., Kreple, C. J., 2013. Acid-sensing ion channels in pain and disease. Nat. Rev. Neurosci. 14, 461–471.

Wu, L. J., Duan, B., Mei, Y. D., Gao, J., Chen, J. G., Zhuo, M., Xu, L., Wu, M., Xu, T. L., 2004. Characterization of acid-sensing ion channels in dorsal horn neurons of rat spinal cord. J. Biol. Chem. 279, 43716-43724.

Xiong, Z.-G., Zhu, X.-M., Chu, X.-P., Minami, M., Hey, J., Wei, W.-L., MacDonald, J. F., Wemmie, J. A., Price, M. P., Welsh, M. J., Simon, R. P., 2004. Neuroprotection in ischemia: blocking calcium-permeable acid-sensing ion channels. Cell 118, 687–698.

Yagi, J., Wenk, H. N., Naves, L. A., McCleskey, E. W., 2006. Sustained currents through ASIC3 ion channels at the modest pH changes that occur during myocardial ischemia. Circ. Res. 99, 501-509.

Yang, L., Palmer, L. G., 2014. Ion conduction and selectivity in acid-sensing ion channel 1. J. Gen. Physiol. 144, 245-255.

Yang, Z. J., Ni, X., Carter, E. L., Kibler, K., Martin, L. J., Koehler, R. C., 2011. Neuroprotective effect of acid-sensing ion channel inhibitor psalmotoxin-1 after hypoxia-ischemia in newborn piglet striatum. Neurobiol. Dis. 43, 446-454.

Young, G. T., Gutteridge, A., Fox, H. D., Wilbrey, A. L., Cao, L., Cho, L. T., Brown, A. R., Benn, C. L., Kammonen, L. R., Friedman, J. H., Bictash, M., Whiting, P., Bilsland, J. G., Stevens, E. B., 2014. Characterizing human stem cell-derived sensory neurons at the single-cell level reveals their ion channel expression and utility in pain research. Mol. Ther. 22, 1530-1543.

Figures

Table 1. Activity summary of ASIC modulators isolated from animal venoms. Values are IC_{50} and EC_{50} values for the rat isoform unless stated otherwise. Activity is colour coded into red, blue, and green indicating **inhibition** ×, **potentiation** ↑, and **agonism** +, respectively.

Peptide	Venom source	Activity
PcTx1	Spider (*Psalmopoeus cambridgei*)	× ASIC1a ~1 and ~3 nM (rat and human) × ASIC1a/2a ~35–85% at 50 nM × ASIC1a/2b ~3 nM ↑ ASIC1b ~100 nM + cASIC1 ~10–189 nM ↑ cASIC1 ~135% at 30 nM
Hm3a	Spider (*Heteroscodra maculata*)	× ASIC1a 1.3 and 39.7 nM (rat and human) ↑ ASIC1b 46.5 and 178 nM (rat and human) ↑ ASIC1a/1b 17.4 nM
APETx2	Sea anemone (*Anthopleura elegantissima*)	× ASIC3 ~60 and 175 nM (rat and human) × ASIC3/1a 2 μM × ASIC3/1b 900 nM × ASIC3/2b 117 nM
Hcr 1b-1	Sea anemone (*Heteractis crispa*)	× ASIC3 5.5 μM (human)
MitTx	Snake (*Micrurus tener tener*)	+ ASIC1a 9 nM + ASIC1b 23 nM ↑ ASIC2a 75 nM + ASIC3 830 nM + cASIC1 ~15% at 300 nM
Ma-1 Ma-2 Ma-3	Snake (*Dendroaspis polylepis polylepis, Dendroaspis augusticeps*)	× ASIC1a 11–55 and 127 nM (rat and human) × ASIC1b 44–192 nM × ASIC1a/1b 72 nM × ASIC1a/2a 252 nM × ASIC1a/2b 61 nM
Ugr 9-1	Sea anemone (*Urticina grebelnyi*)	× ASIC3 10 μM (human, peak) × ASIC3 1.5 μM (human, sustained)
PhcrTx1	Sea anemone (*Phymanthus crucifer*)	× 100 nM (rat sensory neurons)
α-DTx	Snake (*Dendroaspis augusticeps*)	× 800 nM (rat sensory neurons)

Figure 1. ASIC gating conformations, domain organisation, and venom peptide binding sites and functional summary. **(A)** cASIC1 structure in the apo, desensitised state without any peptide bound (PDB code 4NYK; (Gonzales et al., 2009)), with domains of a single subunit within the trimer colour coded. **(B)** The closed state is yet to be solved, and remains one of the biggest unknowns in the ASIC field. **(C)** PcTx1 bound to cASIC1 at low pH (PDB code 4FZ1; (Baconguis and Gouaux, 2012)), and **(D)** MitTx bound to cASIC1 (PDB code 4NTW; (Baconguis et al., 2014)), where both structures were reported at the time of publication to be in the open state. However, there are clear differences in the TM region and it is now thought the MitTx most faithfully represents the Na^+ conductive, proton-gated open state of ASICs. ASIC modulators are shown next to the binding state each peptide favours, for the subtype shown in brackets. ✖ in red indicates inhibitors, ↑ in blue potentiators of pH-gated currents, and + in green direct agonists of the ASIC subtype in brackets for each ligand. Peptide binding sites are in italicised bold, and the grey lines depict the TM region based on the hydrophobicity of the protein surface. Note the functional information listed for each ligand is not complete and is a simplified summary; please refer to the text and Table 1 for more details.

Figure 2. Venom peptide modulators of ASICs. **(A)** Amino acid sequence of venom peptides grouped with homologues where present. Differences in sequences are indicated by grey boxes, and active sites by triangles above the pharmacophore residue. **(B)** Three dimensional structure of PcTx1 (PDB code 2KNI;(Saez et al., 2011)), APETx2 (PDB code 2MUB; (Jensen et al., 2014)), Hi1a (PDB Code 2N8F; (Chassagnon et al., 2017)), Ma-1 (PDB codes 5DU1, 5DZ5; (Mourier et al., 2016)), Ma-2 (PDB code 2MFA; (Schroeder et al., 2014)), MitTx (PDB code 4NTW; (Baconguis et al., 2014)), Ugr 9-1 (PDB code 2LZO; (Osmakov et al., 2013)), and α-DTx (PDB code 1DTX; (Skarżyński, 1992)). All peptides are shown in the same scale and disulfide bonds shown in red. Structures are not available for all peptides and have only been shown where available.

Figure 3. Summary of the active surface of ASIC targeting peptides derived from crystallography and mutagenesis data. (A) Two subunits of cASIC1 are shown as surface representations with the domains colour coded as per Fig. 1. The partially overlapping binding orientations of PcTx1 (grey) and MitTx (blue and cyan) are shown as peptide backbones. The subunit interface corresponding to the acidic pocket is also highlighted. (B) Surface representation of PcTx1 (grey) bound to cASIC1 showing the extensive hydrophobic interaction with α helix 5 (green residues) and the basic residues (blue) that protrude into the acidic pocket. (C) Surface representation of PcTx1 with crystal contact residues highlighted in blue and red. Of these, red represents residues that are the functional pharmacophore and were found to make energetically important interactions for rASIC1a inhibition (these residues are labelled). (D) Active surface of APETx2 for rASIC3 inhibition, mutations of the red residues have a major impact while mutation of the orange had a less severe impact on activity. (E) Active surface of MitTx based on predictions from XRD crystal contacts. (F) Amino acid residues shown to be important for Ma-1 inhibitory activity mapped on to the NMR structure of Ma-2. (NB: structures are not to scale).

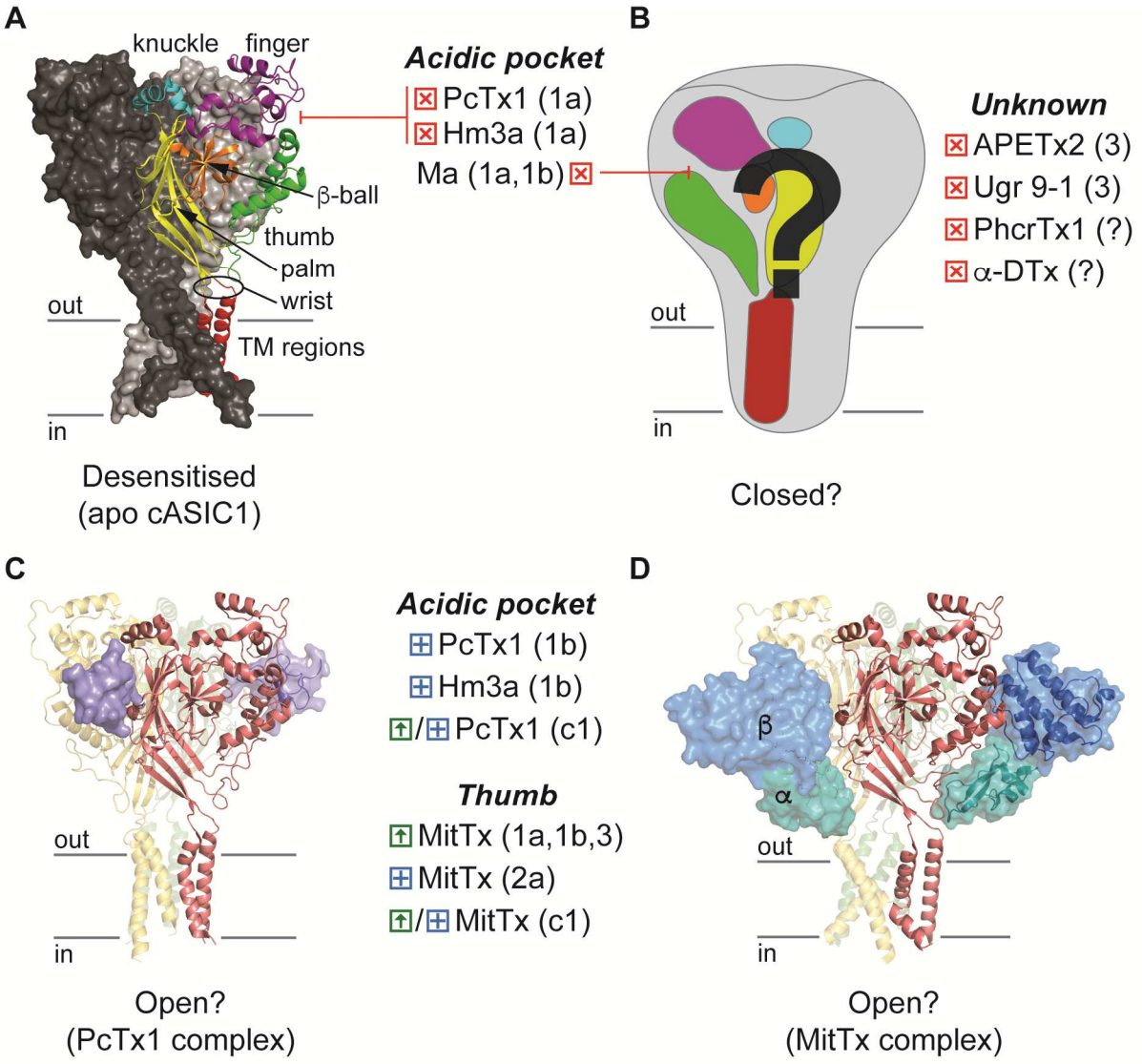
A
knuckle
finger
β-ball
thumb
palm
wrist
out
TM regions
in
Desensitised
(apo cASIC1)
Acidic pocket
PcTx1 (1a)
Hm3a (1a)
Ma (1a,1b)
B
out
in
Closed?
Unknown
APETx2 (3)
Ugr 9-1 (3)
PhcrTx1 (?)
α-DTx (?)
C
out
in
Open?
(PcTx1 complex)
Acidic pocket
PcTx1 (1b)
Hm3a (1b)
PcTx1 (c1)
Thumb
MitTx (1a,1b,3)
MitTx (2a)
MitTx (c1)
D
β
α
out
in
Open?
(MitTx complex)

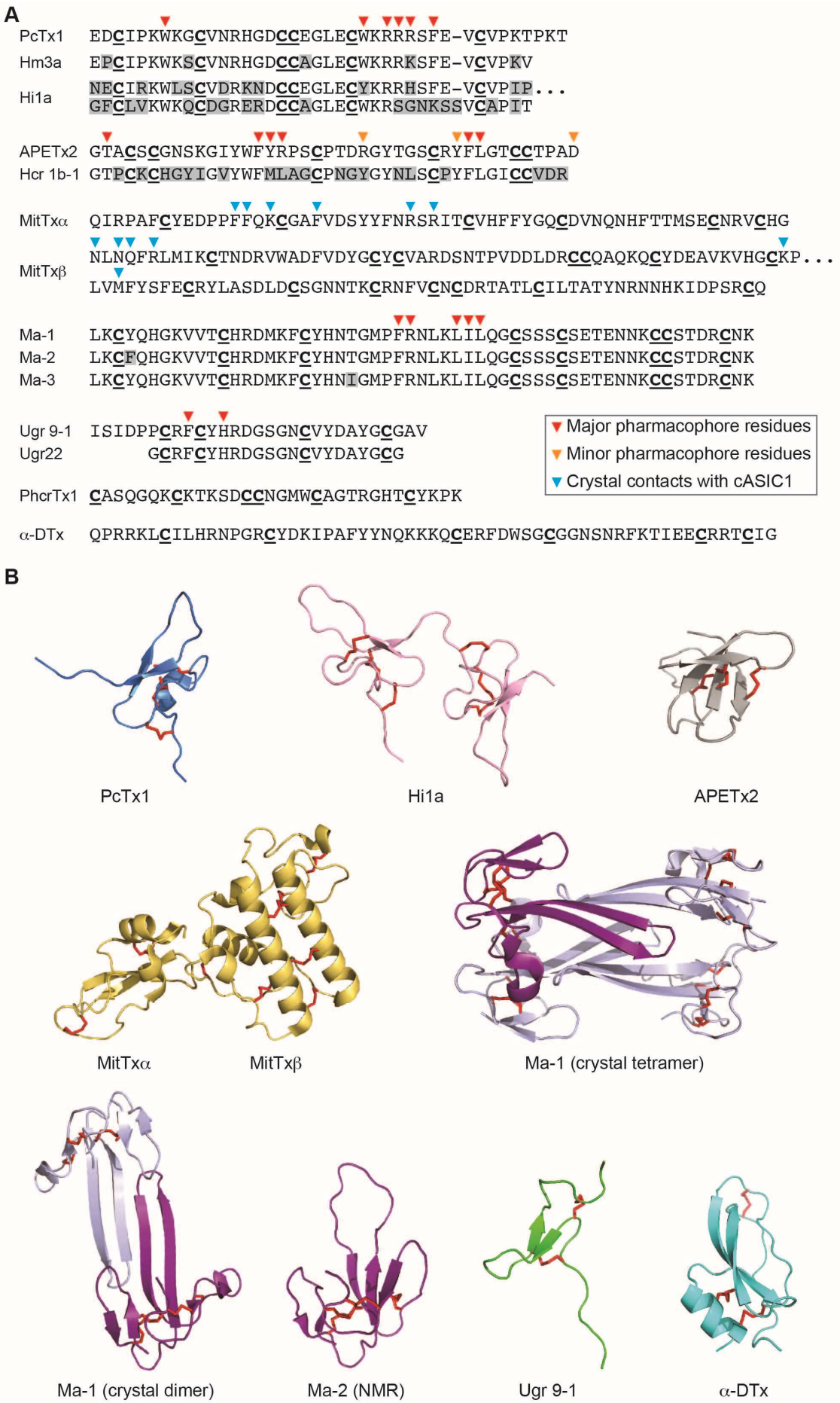
A
PcTx1 EDCIPKWKGCVNRHGDCCEGLECWKRRRSFE-VCVPKTPKT
Hm3a EPCIPKWKSCVNRHGDCCAGLECWKRRKSFE-VCVPKV
Hi1a NECIRKWLSCVDRKNDCCEGLECYKRRHSFE-VCVPIP...
GFCLVKWKQCDGRERDCCAGLECWKRSGNKSSVCAPIT
APETx2 GTACSCGNSKGIYWFYRPSCPTDRGYTGSCRYFLGTCCTPAD
Hcr 1b-1 GTPCKCHGYIGVYWFMLAGCPNGYGYNLSCPYFLGICCVDR
MitTxα QIRPAFCYEDPPFFQKCGAFVDSYYFNRSRITCVHFFYGQCDVNQNHFTTMSECNRVCHG
MitTxβ NLNQFRLMIKCTNDRVWADFVDYGCYCVARDSNTPVDDLDRCCQAQKQCYDEAVKVHGCKP...
LVMFYSFECRYLASDLDCSGNNTKCRNFVCNCDRTATLCILTATYNRNNHKIDPSRCQ
Ma-1 LKCYQHGKVVTCHRDMKFCYHNTGMPFRNLKLILQGCSSSCSETENNKCCSTDRCNK
Ma-2 LKCFQHGKVVTCHRDMKFCYHNTGMPFRNLKLILQGCSSSCSETENNKCCSTDRCNK
Ma-3 LKCYQHGKVVTCHRDMKFCYHNIGMPFRNLKLILQGCSSSCSETENNKCCSTDRCNK
Ugr 9-1 ISIDPPCRFCYHRDGSGNCVYDAYGCGAV
Ugr22 GCRFCYHRDGSGNCVYDAYGCG
PhcrTx1 CASQGQKCKTKSDCCNGMWCAGTRGHTCYKPK
α-DTx QPRRKLCILHRNPGRCYDKIPAFYYNQKKKQCERFDWSGCGGNSNRFKTIEECRRTCIG
Major pharmacophore residues
Minor pharmacophore residues
Crystal contacts with cASIC1
B
PcTx1
Hi1a
APETx2
MitTxα
MitTxβ
Ma-1 (crystal tetramer)
Ma-1 (crystal dimer)
Ma-2 (NMR)
Ugr 9-1
α-DTx

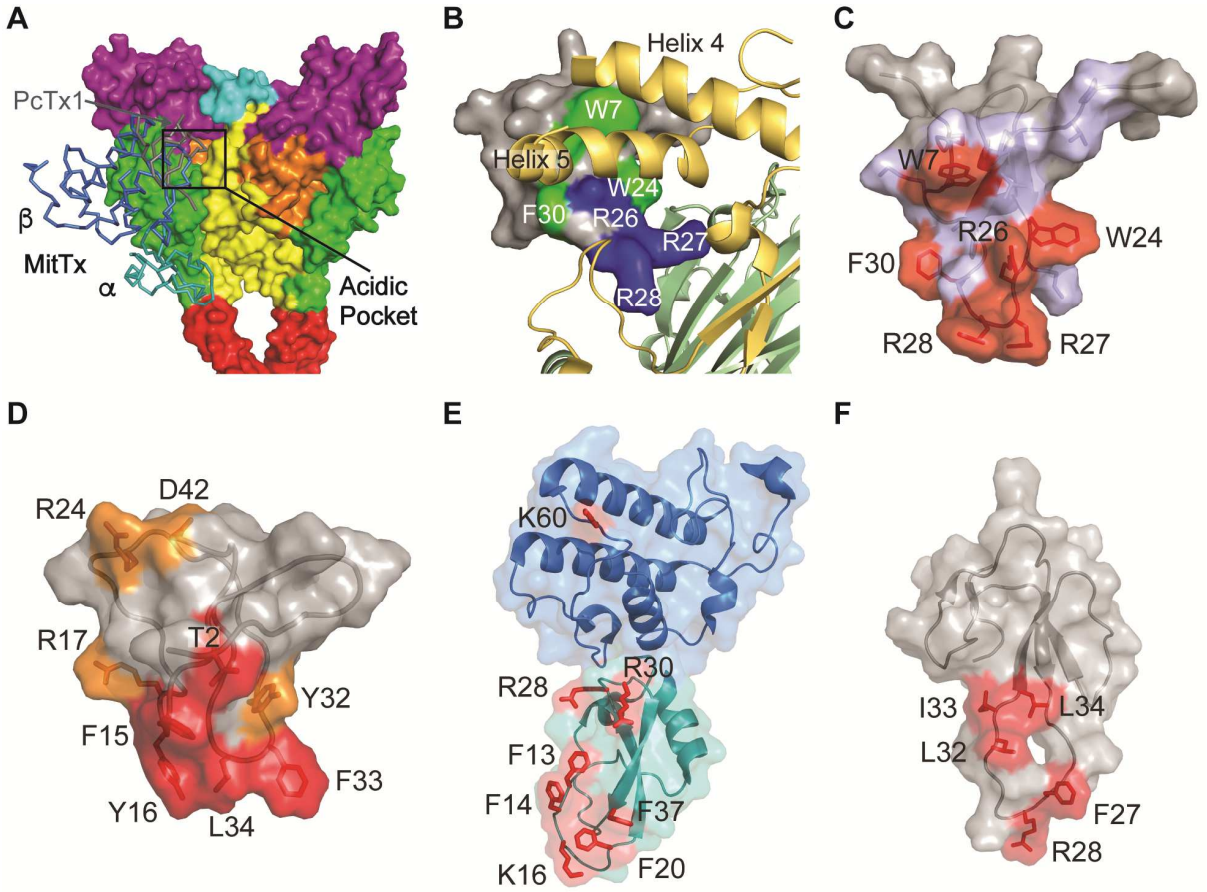

Highlights:

- The most potent and selective modulators of ASICs have come from animal venoms.
- ASIC modulators have been isolated from spiders, sea anemones, and snakes.
- Venom peptides have advanced our understanding of ASIC gating and structure.
- Venom peptides have helped elucidate the *in vitro* and *in vivo* roles of ASICs.
- Venom-derived modulators of ASICs are likely to play a big role in the future.